

# Study of Pattern Recognition in the $\tau \rightarrow \pi^- \pi^+ \pi^- \nu_\tau$ events.

Roberto Della Marina

*I.N.F.N. Sezione di Trieste, Italy*

## Abstract

In this note we present a study of the pattern recognition for the *3-prong*  $\tau$  decays. In many of these events, especially in the case of low neutral reconstructed energy, the *3-prongs* are very collimated in a narrow cone, slightly bended by magnetic field and some of inner sectors coordinates are badly reconstructed. In the following we will describe a procedure to eliminate the bad coordinates and a vertex fit procedure that permits to recover the lost resolution in momentum and mass.

# 1 Introduction

The multi-pion states in  $\tau$  decays give us a good tool to study many aspects of  $\tau$  physics. The study of pattern recognition for these events becomes therefore very important in order to know how well their momentum and energy are reconstructed. We analyzed the 3-prong system of  $\tau$  decays but results apply also to the other multiprong channels: the analysis has been done with 1989-1990 data sample, corresponding to  $8 \text{ pb}^{-1}$ . In this particular topology we achieve some structural limit of our detector:

- When two tracks are very close, TPC reconstructs only one cluster for padrow and JULIA associates it to a intermediate coordinate placed between tracks;
- When two or more tracks pass through a single ITC cell, only one coordinate is reconstructed by “single-hit” ITC electronics: sometimes JULIA associates this coordinate to the wrong track.

Since single track errors are deducted from statistical errors over coordinates, it is clear that, associating a wrong coordinate to a track, we are introducing a systematic error. It is therefore necessary a strong quality check of these quantities and in particular of their errors.

In this note we will analyze in detail the effect of systematic errors in track reconstruction in mass and momentum measurement and we will present a refit procedure, which, using a particular set of “good” coordinates in the track fit, permits to avoid reconstruction ambiguities. Imposing the common vertex position to the refit, it is also possible to improve momentum resolution. This analysis has been developed in my thesis [1].

## 2 Coordinates selection

In order to verify whether systematic effects in pattern recognition are well taken care of, we checked track by track how many coordinates JULIA associates for every pad row. In our situation, the possible setups are four: no reconstructed coordinate per pad row, one, two or three. In the first and the last case we have no information at all or it is complete and it isn't useful to intervene; in the two other cases we checked the distance between these hits and JULIA helixes. For each measured coordinate we extrapolate the three reconstructed tracks on the pad row, it is then possible to calculate  $r\phi$ - and  $z$ - residuals. The three extrapolated tracks have been ordered according to quadratic sum of  $r\phi$ - and  $z$ - residuals. In ideal conditions, first track residuals are both close to 0. In figure 1 and 2 are shown second closer track residuals, in inner and outer sectors respectively (the projections of these plots on  $\Delta r\phi$  and  $\Delta z$  axes are shown in figures 3 and 4). It is noticeable an empty zone for low values of  $\Delta r\phi$  and  $\Delta z$  caused by limited TPC capability in reconstruction of close tracks. It is possible to verify that the bulk of points inside a rectangle with  $\Delta r\phi = 1.7$  and  $\Delta z = 3.0$  sides come from bad reconstructed coordinates when only one cluster has been reconstructed in a middle position between two coordinates. The empty zone in  $\Delta r\phi \sim 0$  and  $2 < \Delta z < 5$  is caused by a cluster overlap: if two tracks overlap in  $r\phi$  and are more than 5 cm (in  $z$ ) away, clusters are well separated and residuals exceed 5 cm. Conversely, if 2 tracks are closer than 5 cm, JULIA

reconstructs often only one cluster in a middle position in  $z$  and residuals will be less than  $2.5\text{ cm}$ . In  $r - \phi$  plane, this effect is much less evident, because track separation depends more strongly from relative position of tracks and pads. It is worthwhile to note that this effect is much more evident in the inner sectors plot, as expected.

In order to be sure that momentum and mass reconstruction are free of pattern recognition systematics, one rejects all coordinates when more than two extrapolated tracks approach within less than  $3\text{ cm}$  in  $z$  and  $1.7\text{ cm}$  in  $r\phi$ . Now it is possible to redo the refit imposing that helixes pass through “safe” coordinates. Because ITC track reconstruction for these events isn’t safe enough, we have chosen to ignore its information. The final result of this “choosing” procedure is that many of inner TPC hits, exactly as ITC coordinates, are lost (see fig. 5 and 6). Imposing to the refit the common decay vertex (the point where  $\tau$  decayed), it is possible to gain again the lost momentum resolution. We estimate the position of this point with the beam interaction point. This estimate is done averaging primary vertex positions in hadronic events and it has little statistical error but a quite important systematic error due to finite dimension of electrons-positrons bunches. These dimensions could be estimated with  $\mu^+\mu^-$  events [2] and it follows:

Dimensions of vertex region		
$x + \Delta x$	$y + \Delta y$	$z + \Delta z$
$156 \pm 4\ \mu m$	$33 \pm 12\ \mu m$	$9.85 \pm 0.12\ mm$

Table 1: Dimensions of primary vertex luminous region calculated with 1990  $\mu^+\mu^-$  events.

In order to take care of non-pointlike interaction region, it is necessary to do again the refit moving the vertex to the edges of the luminous region ( $\Delta x, \Delta y, \Delta z$ ). The absolute value of resulting variations, obtained moving the vertex, estimates the error in energy. These variations are identical in momentum and opposite in sign moving the vertex along an axis first in one direction and then in the opposite one. In the fit it is necessary to take into account the finite  $\tau$ -lifetime effect ( $2 - 3\text{ mm}$  free path). This is obtained displacing by  $4\text{ mm}$  the vertex in the direction of the reconstructed momentum (the sum of the three momenta of the three pions).

### 3 Check of refitting procedure with Monte Carlo $\tau^+\tau^-$ events

A complete study of systematics that are correlated with the refitting procedure has been done with Monte Carlo  $e^+e^- \rightarrow \tau^+\tau^-$  events. The first result we got, is that well separated tracks are not improved by the refit: the main goal is to improve reconstruction of confused tracks. In figure 7 it is shown the difference between  $3\text{-prongs}$  reconstructed energy and “true” energy of 1658 Monte Carlo events in 3 possible fit setups:

1. Standard JULIA fit using both ITC and TPC information;
2. Fit choosing coordinates using only TPC information;
3. Fit choosing coordinates using only TPC information and imposing the vertex.

These plots show that the new refit does not introduce evident systematics: in all occurrences, the mean value is well near 0. In the first plot is shown the distribution of  $E_{3prong} - E_{true}$  obtained with standard JULIA fit with  $\sigma^2 = 1.16 \text{ GeV}^2$  and 8 events out of picture (6 in overflow and 2 in underflow). Excluding from refit ITC and bad reconstructed coordinates, the dispersion of reconstructed energy gets bigger ( about 40%,  $\sigma^2 = 1.89$ ), as expected. Imposing the vertex, the mean squared error decreases ( $\sigma^2 = 0.69$ ) as well as distributions tails (10 events in underflow or in overflow). This implies that the vertex refit reduces tails and gains again momentum resolution, that was lost excluding coordinates.

For our analysis it is fundamental that error on reconstructed energy must be correctly evaluated. This error changes event by event: the right variables to study in order to emphasize the rightness of error determination is:

$$\frac{E_{reconstructed} - E_{true}}{\Delta E} \quad (1)$$

where  $\Delta E$  is the error over energy measurement estimated with our procedure. In plot 8 it is possible to note that a gaussian curve fits very well the distribution and it follows that, within 20%, errors are well reconstructed. 36 events remain out of  $\pm 3\sigma$  indicating that this phenomenon interests less than 2% of total sample.

In plot 9 it is shown the plot of  $\Delta E$  for data and Monte Carlo: notice the nice agreement. The mean value of this error is 400 MeV. Analysing the mass reconstruction with a similar procedure it follows for the error on reconstructed mass a value of 17 MeV/c<sup>2</sup>.

In plots 10 and 11 are shown different contributions to energy total error: typical values are 300 MeV for statistical error, 200 MeV moving the vertex by  $\sigma_x$ , 40 MeV moving it by  $\sigma_y$  and 100 MeV moving it by  $\sigma_z$ . The  $\tau$  lifetime contribution to systematic error on energy is about 30 MeV. The smallness of this error is due to the fact that, moving a point along the fitted helix, doesn't change track's momentum : if one moves the decay vertex in the direction of visible momentum get a similar effect.

In this paragraph we showed that on Monte Carlo events the refitting procedure gives reasonably accurate errors: the next step is to look at other physical processes for a hint for the value of this error on data. A nice  $Z^0$  decay channel that is useful for our purposes is  $e^+e^- \rightarrow \mu^+\mu^-$ , where "true"  $\mu$  energy can be well estimated with beam energy and the (1) is applied to real events where  $E_{beam}$  takes the place of  $E_{true}$ .

## 4 Check of energy resolution with $\mu^+\mu^-$ events

In the previous paragraph it is shown that, excluding shared or bad reconstructed coordinates from the fit of 3-prongs tracks, it is possible to reproduce "isolated track" conditions. In this hypothesis, the statistical error that JULIA quotes for every track fit, is properly evaluated. An easy way to check it, is to process  $\mu^+\mu^-$  events with the refitting procedure.

The selection of  $\mu^+\mu^-$  events used for this check, is done with the following requirements:

1. Two tracks of opposite charge, one for each hemisphere;
2. Acollinearity best than  $\cos \eta_{acol} = -0.9975$ ;
3. Total reconstructed ECAL energy less than  $2 \text{ GeV}$ ;
4. One track with momentum greater than  $42 \text{ GeV}/c$ .

The track on which momentum cut (cut 4) has to be applied, is randomly selected and the analysis is done on the other track: in this way, using beam energy in order to estimate the “true” energy, no bias at all is introduced. The cuts 2 and 3 assure that there are no big initial or final state radiation effects: this is important because the hypothesis to estimate the “true” energy with beam energy will be correct. In figures 12, 13 and 14 are shown refit results on  $\mu^+\mu^-$  events compared with standard JULIA fit in following configurations:

- Standard JULIA fit;
- Vertex fit taking into account finite dimensions of luminous region;
- Vertex fit taking into account finite dimensions of luminous region and outer TPC coordinates only.

The last option would like to simulate as well as possible *3-prong*  $\tau$  decay, where outer TPC coordinates only are “good” coordinates. We made two tests: the first one on Monte Carlo  $\mu^+\mu^-$  events and the other one on the data sample. In figure 12 (Monte Carlo) are shown the results of these three fits obtained with the same procedure used in the previous paragraph. In figure 13, incoming electron energy has been used instead of  $E_{true}$ : results are clearly consistent. The results of refit on data are shown in figure 14: in this case also the refit works well and it is possible to conclude that the estimate of errors is correct also in data. In figure 15 is shown the comparison between data and Monte Carlo estimates of total error on energy, done imposing the vertex to the fit, excluding ITC and outer TPC coordinates and asking for tracks well contained in the TPC ( $|\cos \theta| < 0.8$ ): the matching between distributions is good and it is remarkable that the mean value of the error ( $\simeq 1.6 \text{ GeV}$ ) corresponds to  $\frac{\Delta p}{p} \simeq 3.5\%$ . At  $45 \text{ GeV}$  that gives  $\frac{\Delta p}{p^2} \simeq 0.8 \times 10^{-3} (\text{GeV}/c)^{-1}$ , which corresponds to standard ITC+TPC resolution [3]: it follows that, excluding ITC hits and first nine TPC rows, the refit with vertex doesn’t lower resolution.

It is also interesting to verify the absolute momentum scale in the TPC. Using the same  $\mu^+\mu^-$  data sample, we plot  $1 - \frac{E_\mu}{E_{beam}}$  for both Monte Carlo and data (see fig. 19). The central value of the gaussian fit to the data is  $0.0026 \pm 0.0006$  rather different to 0. We cannot attribute this difference to the energy scale, because in our selection we are not able to check the initial or final state radiated energy in the scale of the observed shift (the shift corresponds to a radiation energy loss of about  $170 \text{ MeV}$  per event). The mean value of the Monte Carlo distribution is  $0.0023 \pm 0.0009$  and shows that the shift from 0 is mostly due to radiation effects. The differences between the two mean values is  $0.0003 \pm 0.0010$  and shows that the TPC energy scale is correct within 0.1%. It is

remarkable to notice that this result has been obtained in ALEPH without calibrating the TPC energy scale with the events themselves.

Finally, it is useful to analyse track  $\chi^2$ . Looking into distributions plotted in figures 13 and 14 for  $\mu^+\mu^-$  events, there are evident some tails beyond  $3\sigma$  from distribution central value. If we plot event by event the  $\chi^2$  normalized to degrees of freedom of the tracks fit (see fig. 16), it is evident that tails could be strongly reduced imposing:

$$\frac{\chi^2}{N_{d.o.f.}} < 3.$$

We decide to implement this cut in  $\tau$  events also, in order to maintain high precision in momentum measurements (see fig. 17).

In conclusion, in figure 18 we show the comparison between  $\chi^2/N_{d.o.f.}$  distribution for Monte Carlo and data sample of  $\beta$ -prony  $\tau$  events: the behavior is identical but we could note that the cut effect is bigger for data than for Monte Carlo.

## 5 Conclusions

In this note, we showed a safe track refit procedure that permits to control momentum reconstruction, especially regarding his errors due to wrong coordinate to track association. It is shown that imposing the common vertex to the track fit after the “choosing” procedure, it is possible to keep the design ITC+TPC momentum resolution, throwing out “bad” or “unsafe” coordinates.

## References

- [1] R.Della Marina  
“Limiti sulla massa del neutrino  $\nu_\tau$  con l'apparato ALEPH”  
Tesi di laurea. Trieste, December 1991, unpublished.
- [2] S.Wasserbaech  
“Size of the Luminous Region at LEP Interaction point 4”  
ALEPH *internal report* ALEPH 91-57 (1991).
- [3] AA. VV. (ALEPH coll.)  
“Performance of the ALEPH Time Projection Chamber”  
CERN *preprint* CERN-PPE/91-24 (1991).

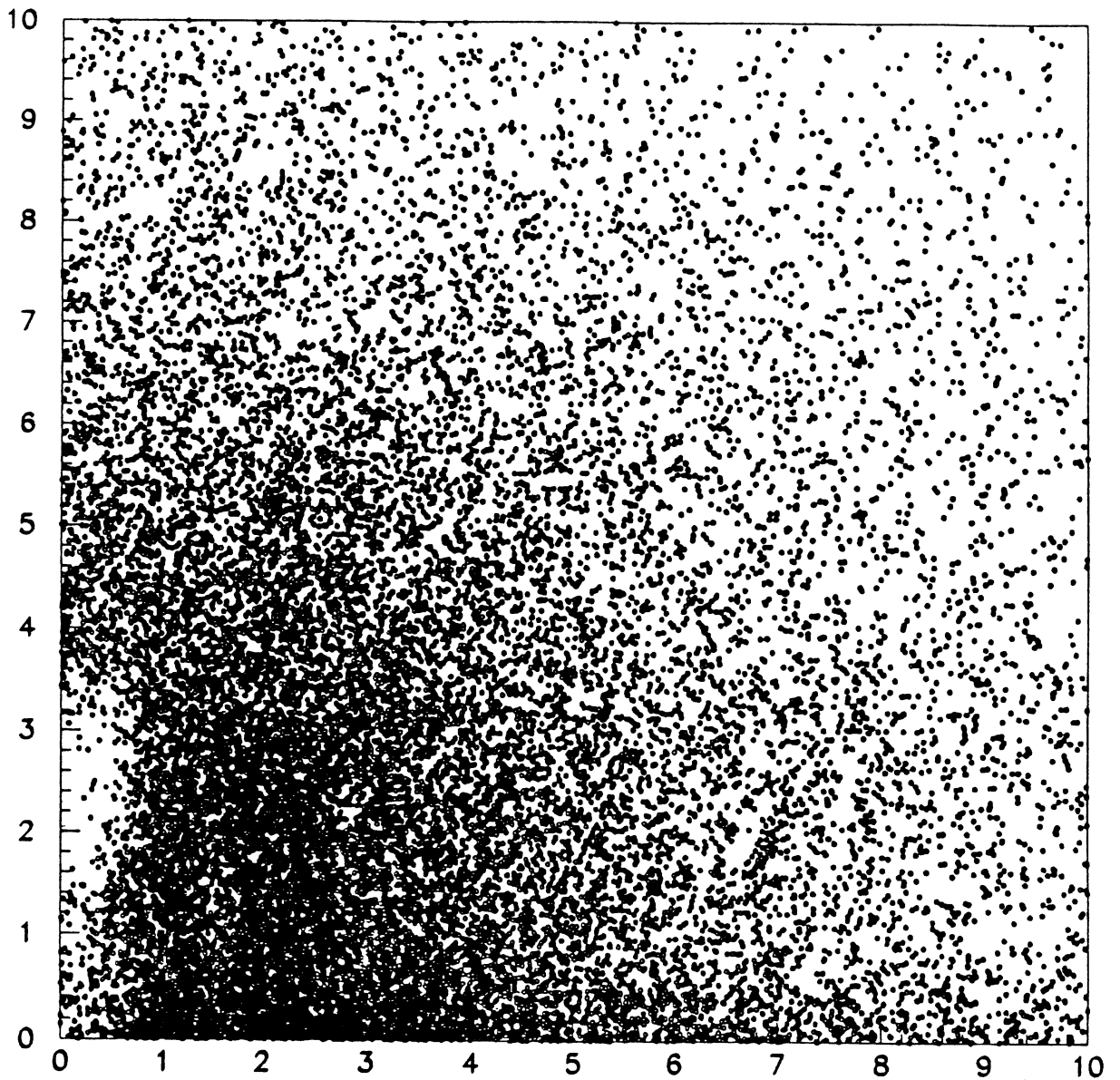


Figure 1: Plot of  $r\phi$  e  $z$  residuals for the second closer track to a hit in the first 9 TPC pad rows.

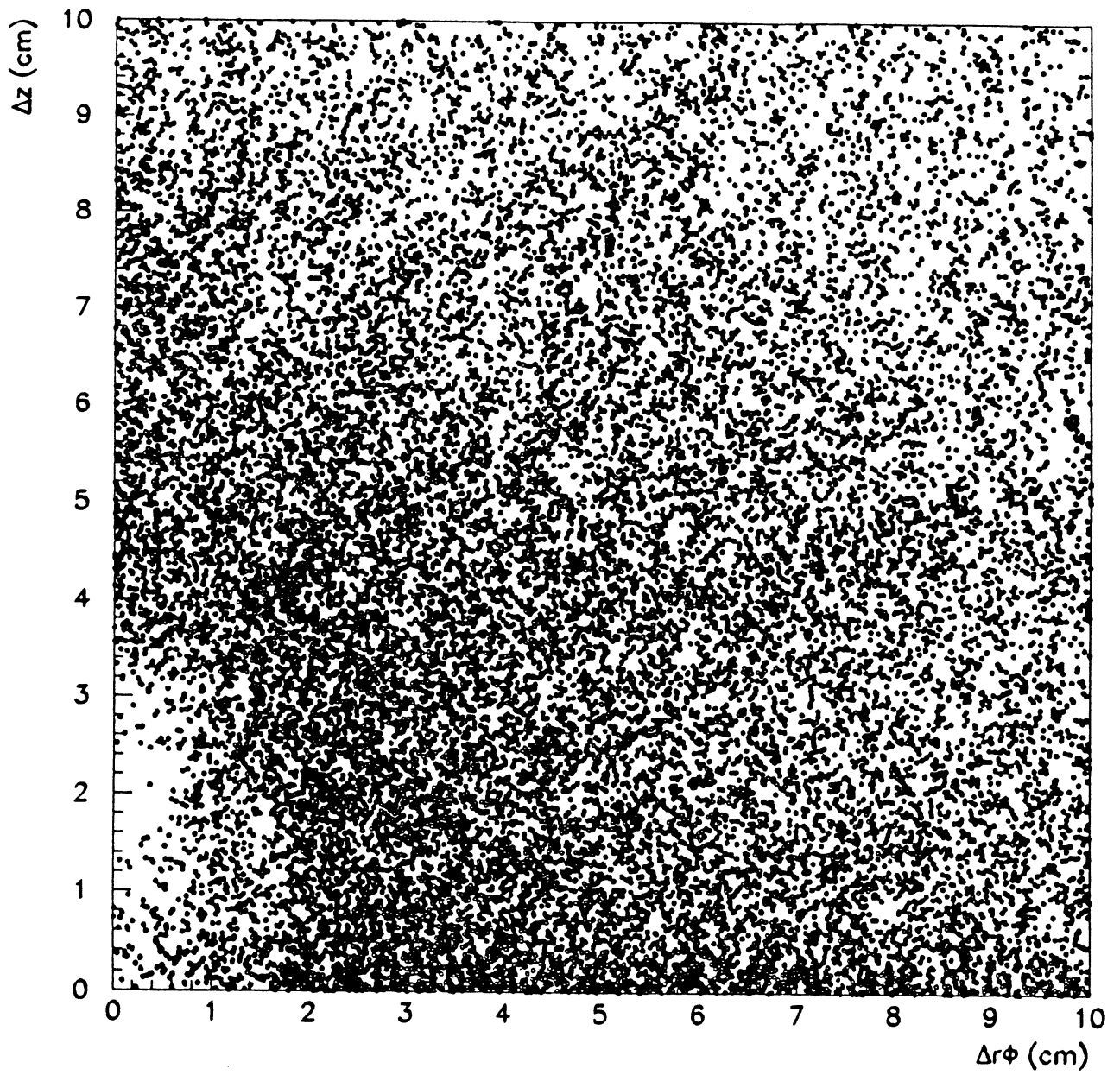


Figure 2: Plot of  $r\phi$  e  $z$  residuals for the second closer track to a hit in external TPC pad rows.



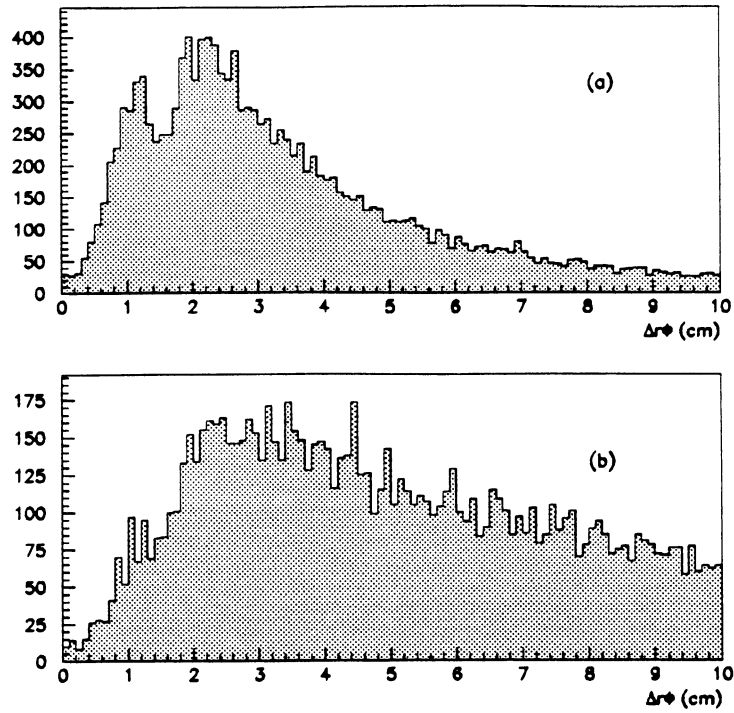


Figure 3: Plot of  $\Delta r\phi$  projections of residuals for the second closer track to a hit in the TPC in: (a) inner sectors (b) outer sectors.

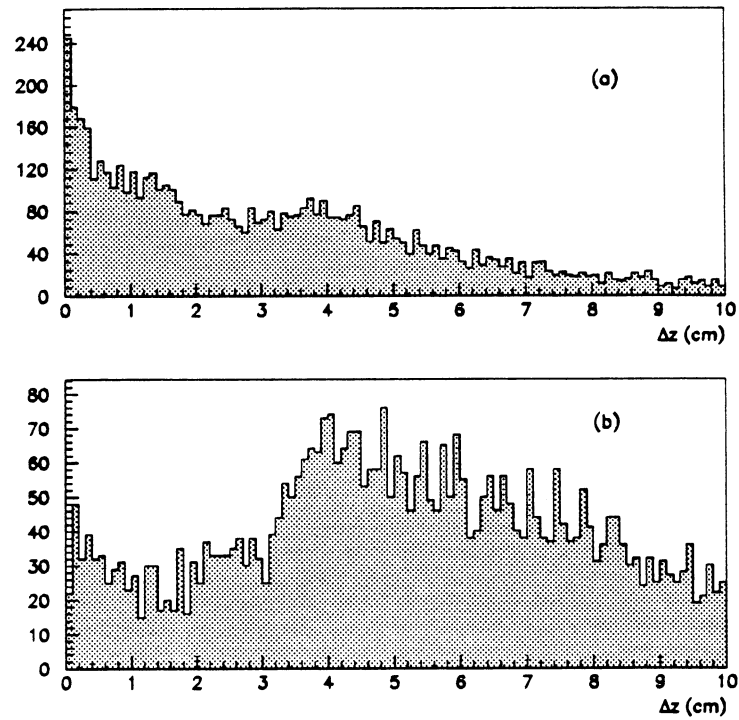


Figure 4: Plot of  $\Delta z$  projections of residuals for the second closer track to a hit in the TPC in: (a) inner sectors (b) outer sectors.

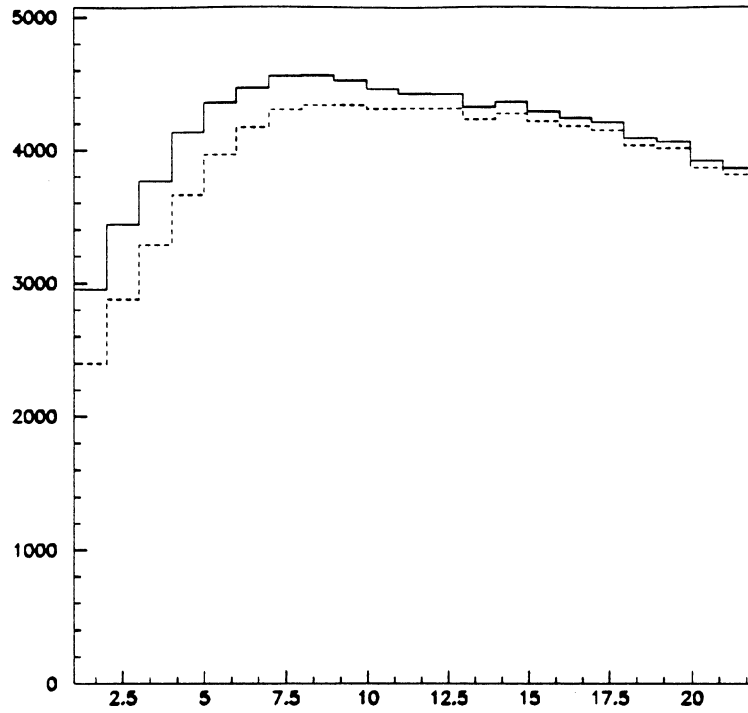


Figure 5: Plot of total number of coordinates for every pad row before (solid line) e after (dotted line) “choosing” procedure.

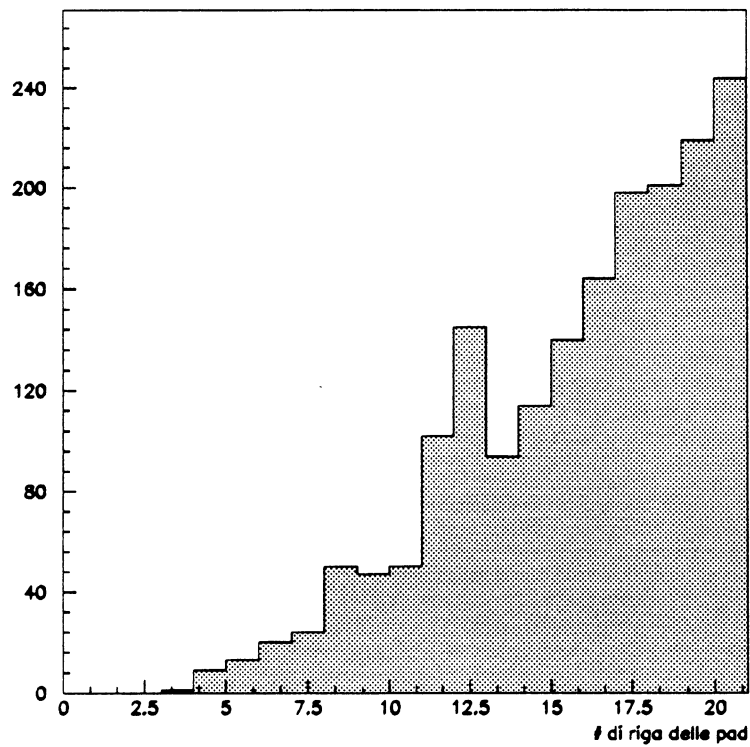


Figure 6: Number of TPC hits for every reconstructed track after “choosing” procedure.

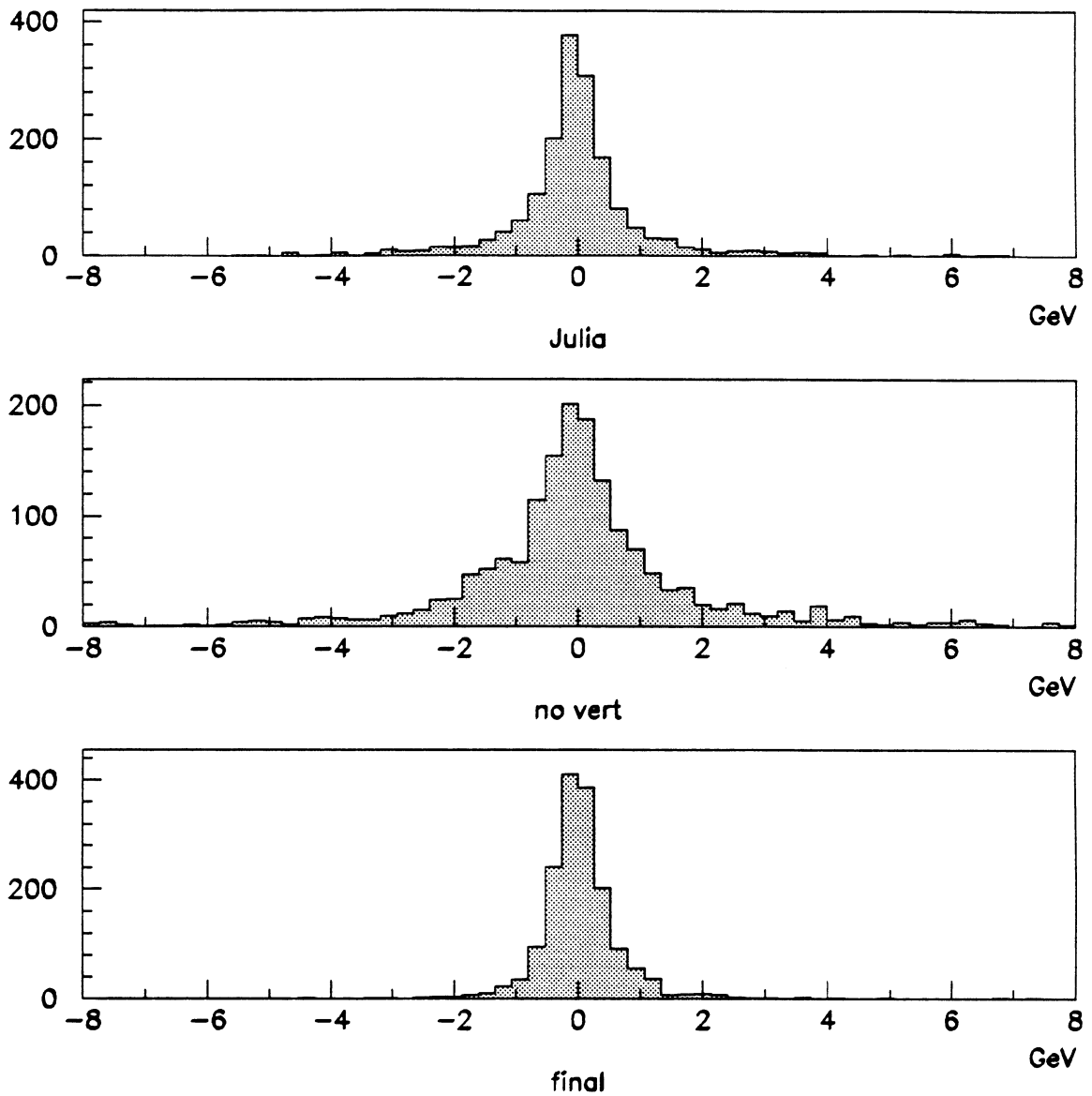


Figure 7: Comparison among fit results with Monte Carlo events. In the plot are shown  $E_{3prong} - E_{true}$  for: (a) Standard JULIA fit; (b) Fit choosing coordinates using only TPC information; (c) Fit choosing coordinates using only TPC information and imposing the vertex.

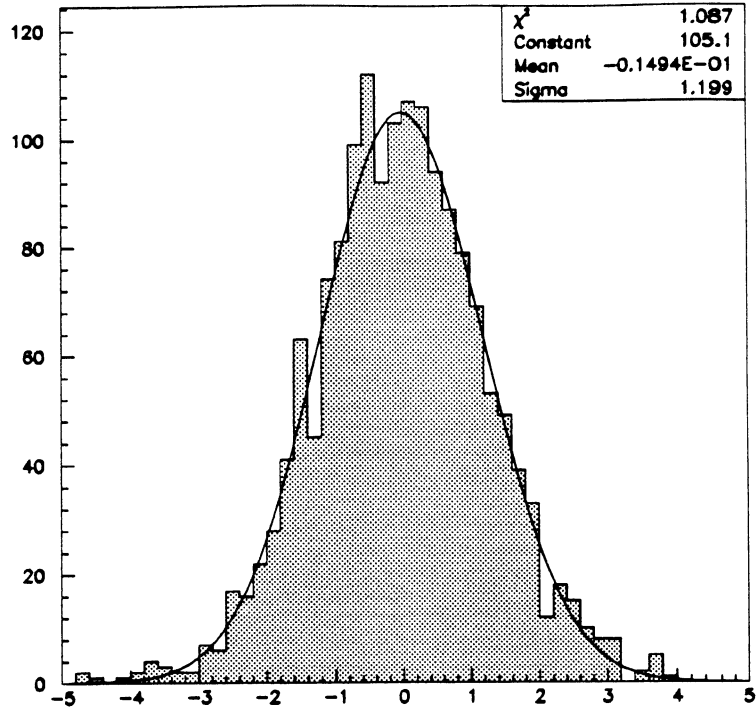


Figure 8: Plot of  $(E_{3prong} - E_{true})/\sigma$  from Monte Carlo  $\tau$  events. The RMS obtained from gaussian fit gives the weight for errors over energy in data sample.

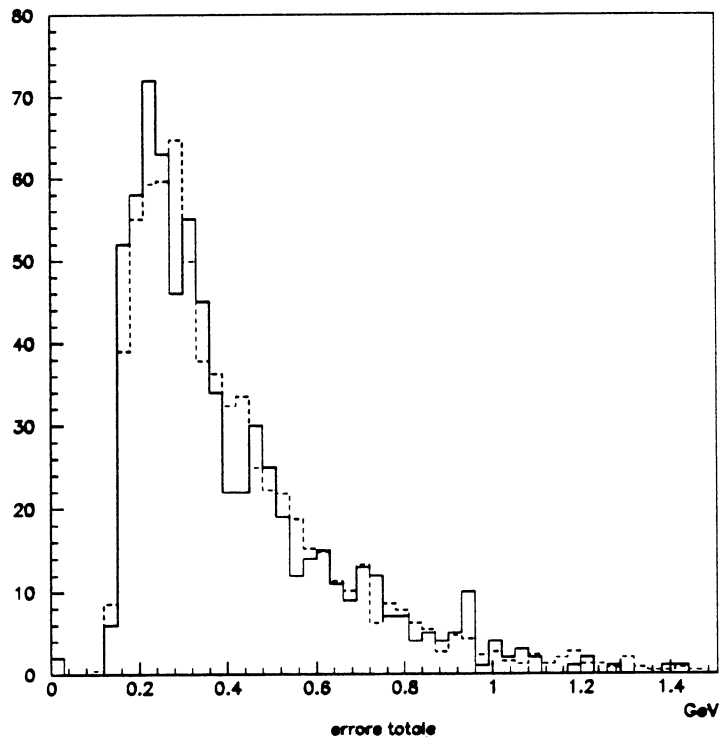


Figure 9: Comparison between  $\tau$  Monte Carlo (dotted line) and data (solid line) energy total error of 3-prong system.

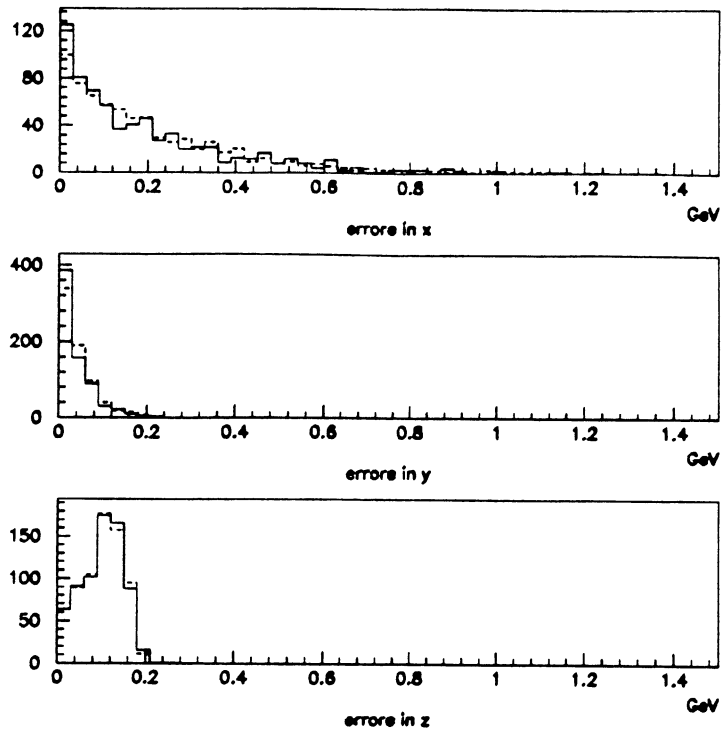


Figure 10: Plot of contributions to systematic error on  $\mathcal{B}$ -prongs energy due to vertex position movement:  $156 \mu\text{m}$  in  $x$  (top),  $33 \mu\text{m}$  in  $y$  (center) e  $9.85 \text{ mm}$  in  $z$  (bottom). In the plot is shown the comparison between Monte Carlo (dotted line) and data (solid line).

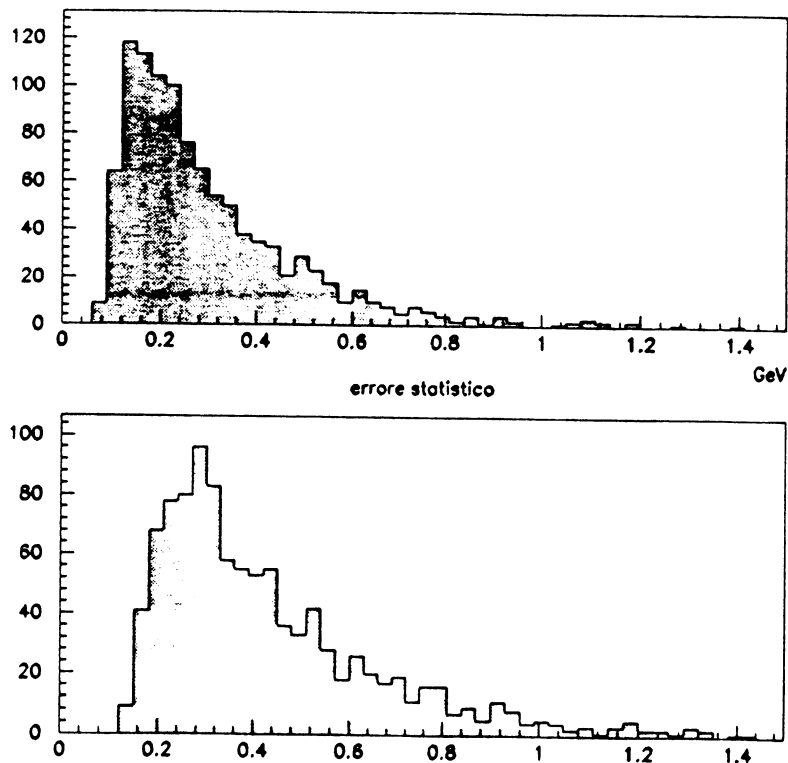


Figure 11: Plot of error on energy for  $\tau$  Monte Carlo  $\mathcal{B}$ -prongs events. In the plot are shown statistical error behaviour (top) and total error behaviour (bottom).

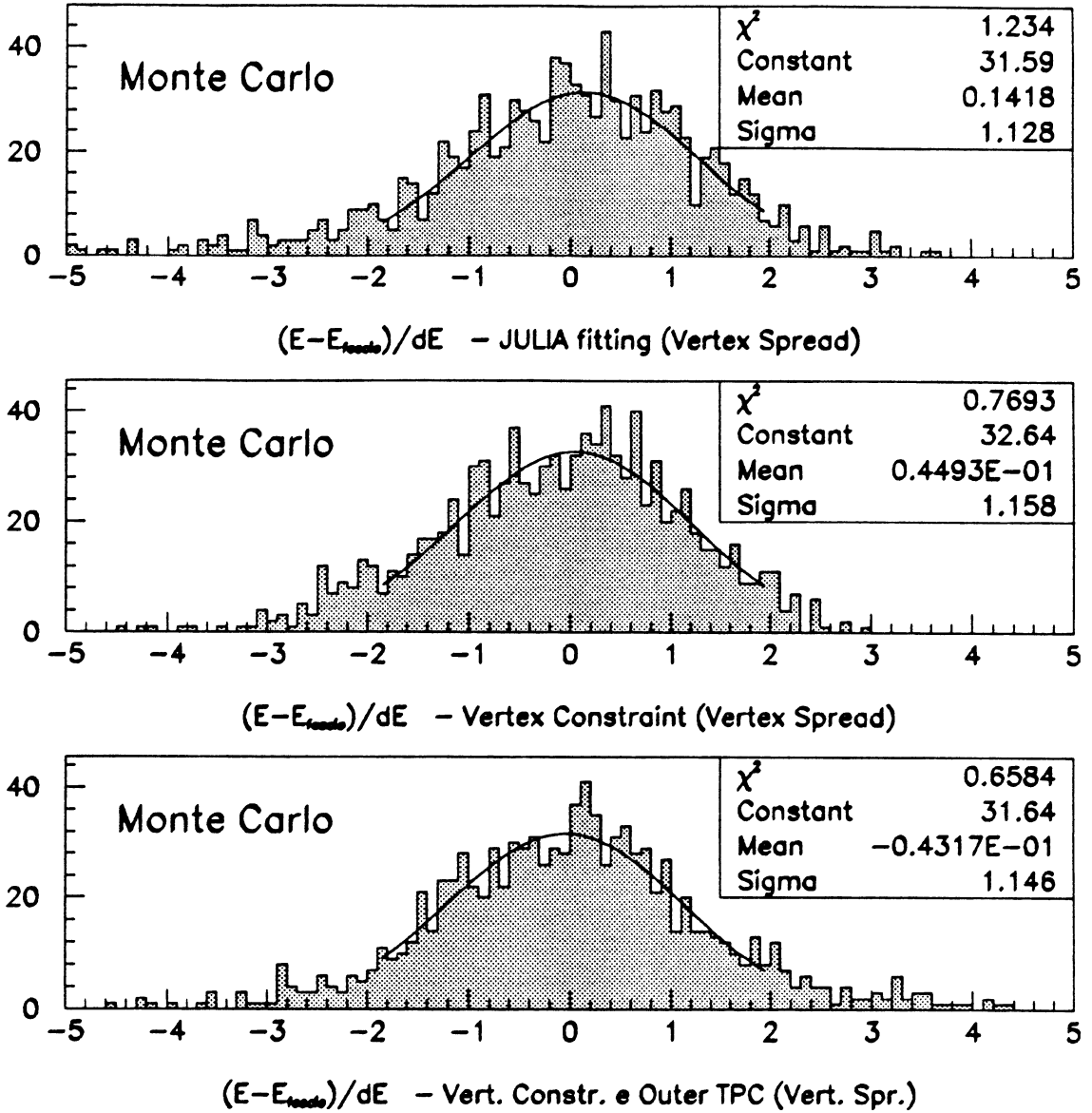


Figure 13: Plot of  $(E_\mu - E_{beam})/\sigma$  from  $\mu^+\mu^-$  Monte Carlo events. In the plot is show the comparison among following settings: (a) Standard JULIA fit; (b) Vertex fit encountering finite dimensions of luminous region; (c) Vertex fit encountering finite dimensions of luminous region and outer TPC coordinates only.

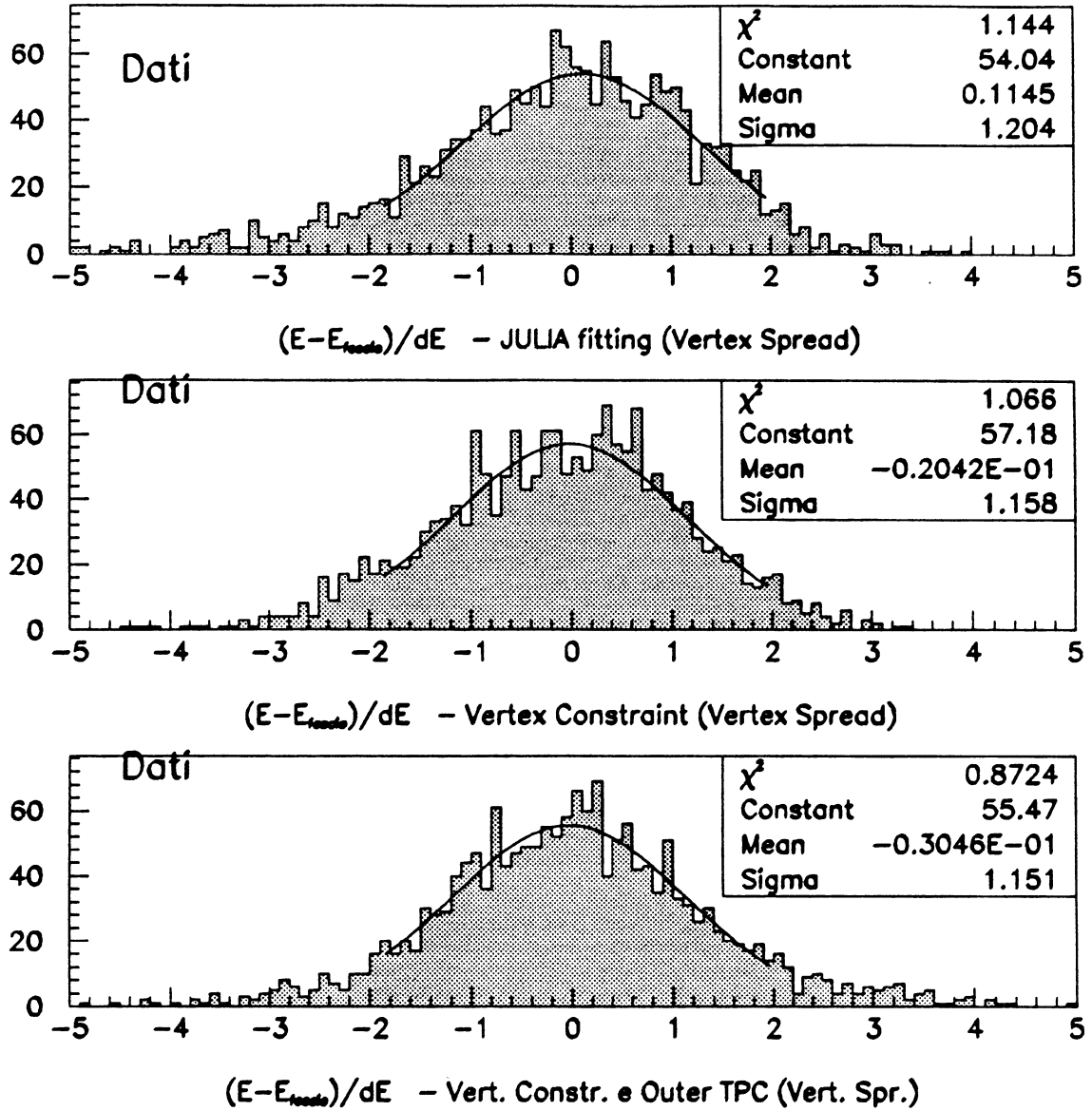


Figure 14: Plot of  $(E_\mu - E_{beam})/\sigma$  from data's  $\mu^+\mu^-$  events. In the plot is show the comparison among following settings: (a) Standard JULIA fit; (b) Vertex fit encountering finite dimensions of luminous region; (c) Vertex fit encountering finite dimensions of luminous region and outer TPC coordinates only.

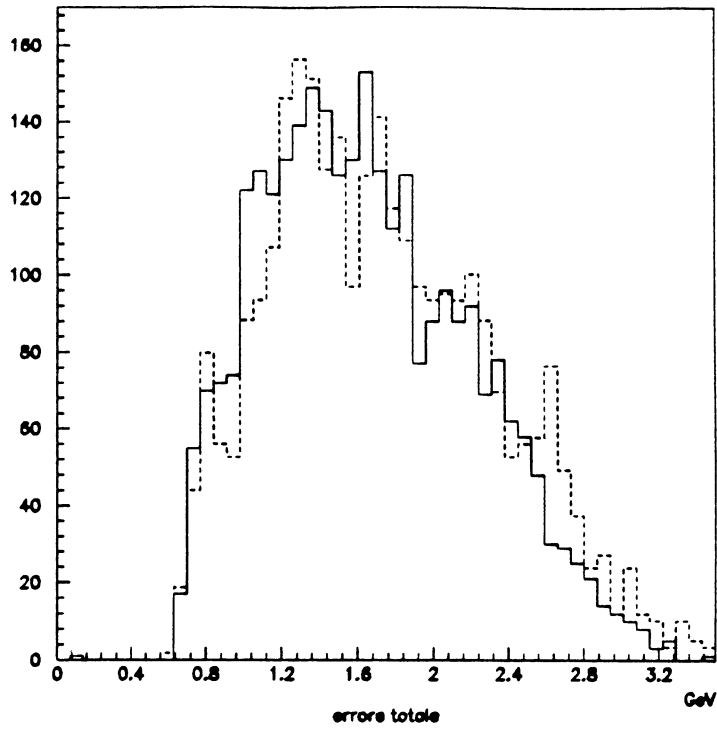


Figure 15: Comparison between energy total error for  $\mu^+\mu^-$  Monte Carlo (dotted line) and data(solid line).

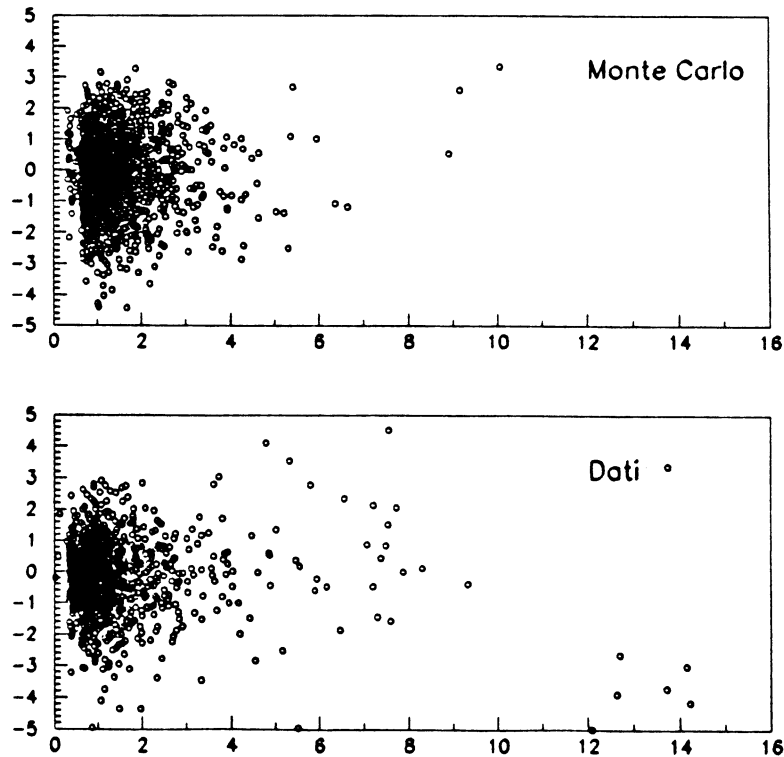


Figure 16: Plot of  $\chi^2/N_{d.o.f.}$  versus  $(E_\mu - E_{beam})/\sigma$  for  $\mu^+\mu^-$  events after refitting. In the plot are shown Monte Carlo events (top) and data(bottom).



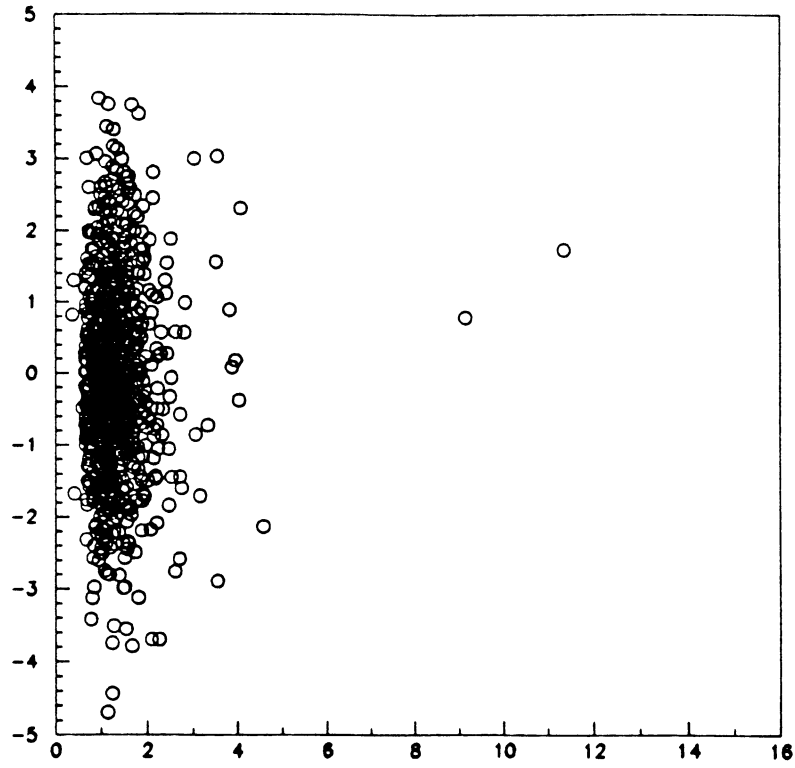


Figure 17: Plot of  $\chi^2/N_{d.o.f.}$  versus  $(E_{3prong} - E_{beam})/\sigma$  for Monte Carlo  $\tau$  events after refitting.

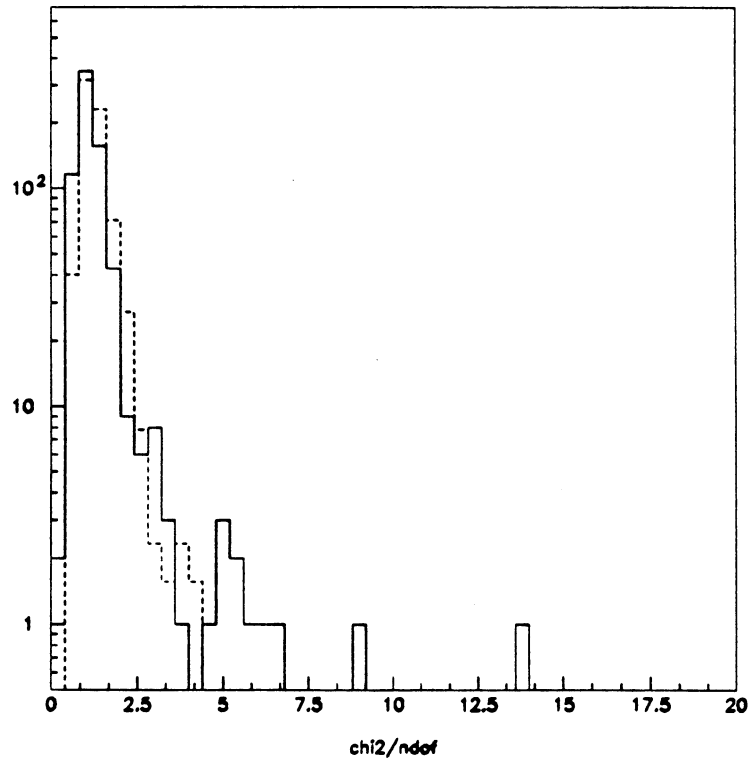


Figure 18: Comparison between  $\chi^2/N_{d.o.f.}$  for  $\tau$  Monte Carlo (dotted line) and data (solid line) events.

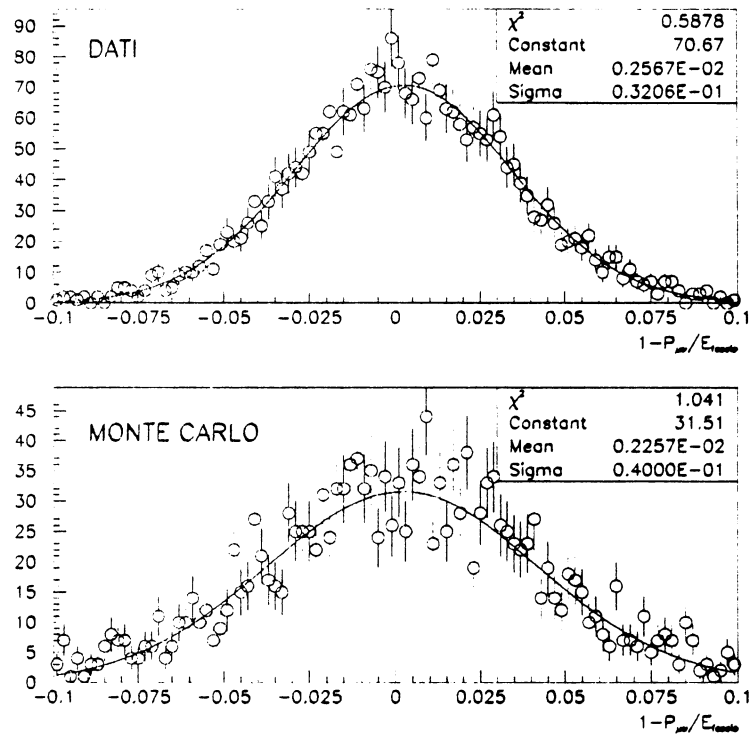


Figure 19: Distribution of  $1 - E_{\mu} / E_{beam}$  in the selected  $Z^0 \rightarrow \mu^+ \mu^-$  events. The gaussian fit results are superimposed to histograms.